Neutrinoless double-β decay of ^{76}Ge: First results from the International Germanium Experiment (IGEX) with six isotopically enriched detectors

C. E. Aalseth,[1] F. T. Avignone III,[1] R. L. Brodzinski,[2] J. I. Collar,[1,*] E. Garcia,[3] D. González,[3] F. Hasenbalg,[1,†] W. K. Hensley,[2] I. V. Kirpichnikov,[4] A. A. Klimenko,[5] H. S. Miley,[2] A. Morales,[3] J. Morales,[3] A. Ortiz de Solórzano,[3] S. B. Osetrov,[5] V. S. Pogosov,[6] J. Puimedón,[3] J. H. Reeves,[2] A. Salinas,[3] M. L. Sarsa,[3,‡] A. A. Smolnikov,[5] A. S. Starostin,[4] A. G. Tamanyan,[6] A. A. Vasenko,[4] S. I. Vasiliev,[5] and J. A. Villar[3]

[1]*University of South Carolina, Columbia, South Carolina 29208*

[2]*Pacific Northwest National Laboratory, Richland, Washington 99352*

[3]*University of Zaragoza, 50009 Zaragoza, Spain*

[4]*Institute for Theoretical and Experimental Physics, 117259 Moscow, Russia*

[5]*Institute for Nuclear Research, Baksan Neutrino Observatory, 361609 Neutrino, Russia*

[6]*Yerevan Physical Institute, 375 036 Yerevan, Armenia*

(The IGEX Collaboration)

(Received 25 June 1998)

The International Germanium Experiment (IGEX) has six HPGe detectors, isotopically enriched to 86% in ^{76}Ge, containing approximately 90 active moles of ^{76}Ge. Three detectors of 2 kg each operate in the Canfranc Underground Laboratory (Spain) with pulse-shape analysis electronics. One detector ($\sim$0.7 kg active volume) has been operating in the Baksan Low-Background Laboratory for several years, and two additional similar detectors will operate in Baksan. A maximum likelihood analysis of 74.84 active mole years of data yields a lower bound $T^{0\nu}_{1/2} \geq 0.8\times 10^{25}$ yr (90% C.L.), corresponding to $\langle m_\nu \rangle < (0.5-1.5)$ eV, depending on the theoretical nuclear matrix elements used to extract the neutrino mass parameter. [S0556-2813(99)01604-0]

PACS number(s): 23.40.−s, 14.60.Pq, 27.50.+e

I. INTRODUCTION

In the standard model of particle physics neutrinos are strictly massless, although there is no theoretical reason for such. On the experimental side, there is no compelling evidence that neutrinos have nonzero masses, although the results of several experiments with solar, atmospheric, and terrestrial neutrinos lead to inconsistencies in the standard theory, unless it is assumed that neutrinos indeed have mass(es).

The anomalous electron to muon ratio observed in underground experiments on atmospheric neutrinos in Soudan and Kamioka, the solar neutrino deficit seen in the Homestake, SAGE, GALLEX, Kamiokande, and Superkamiokande experiments, and the excess electron events seen in the Liquid Scintillator Neutrino Detector (LSND) experiment at Los Alamos could all be explained within the frame of neutrino oscillations. This scenario requires nonzero neutrino masses and mixing between the various neutrino flavors.

Dark matter models of galaxy formation, which have $\sim$75% nonbaryonic cold dark matter, 20% hot dark matter, and 5% dark baryons, fit a large body of data rather well, properly matching observed spectral power at all scales of the universe. A light neutrino could constitute hot dark matter and at the same time solve the neutrino oscillation problem if it has a mass of a few eV.

In the standard model it is assumed that neutrinos and antineutrinos are different particles, but no experimental proof exists thus far. Nuclear double-β-decay experiments address the following questions: (1) are neutrinos self-conjugate and (2) do they have Majorana mass? Various theoretical neutrino mass scenarios reconcile both the matter and vacuum oscillation solutions of the solar neutrino problem and allow the possibility of neutrinoless double-β decay with an effective Majorana neutrino mass in the range of 0.1–1 eV, the target sensitivity of IGEX.

II. DOUBLE-β DECAY

Neutrinoless $\beta\beta$ decay is the only practical way to determine if neutrinos are Majorana particles. In an extension of the black-box theorem of Schechter and Valle [1], Kayser, Petkov, and Rosen showed that in the context of any gauge theory, the observation of 0ν $\beta\beta$ decay would constitute unambiguous evidence that at least one neutrino eigenstate has nonzero mass [2]. In the standard model, weak interactions preserve lepton number exactly, whereas neutrinoless $\beta\beta$ decay would violate it. Additionally, a neutrinoless decay mode could reveal the existence of majorons, scalar Goldstone bosons that result from a spontaneous symmetry breaking mechanism that results in the generation of neutrino mass. These and other features make the search for neutrinoless double-β decay invaluable for exploring non-standard-model physics.

The transition probability of the lepton number violating 0ν $\beta\beta$ decay driven by a Majorana neutrino mass term is expressed as [3]

*Present address: PPE Division, CERN, Geneva 23, Switzerland.

†Present address: Universitaet Bern, CH-3012 Bern, Switzerland.

‡Present address: TUM, Garching, Germany.

TABLE I. Theoretical nuclear structure factors F_N and Majorana neutrino mass parameters corresponding to $T^{0\nu}_{1/2}=10^{25}$ yr.

F_N (yr)$^{-1}$	Model	$\langle m_\nu\rangle$ eV	Reference
1.56×10^{-13}	Weak coupling shell model	0.41	[12]
9.67×10^{-15}	QRPA	1.69	[14], [15]
1.21×10^{-13}	QRPA	0.47	[16]
1.12×10^{-13}	QRPA	0.48	[17]
1.41×10^{-14}	Shell model	1.36	[13]

$$[T^{0\nu}_{1/2}(0^+\rightarrow0^+)]^{-1}=G_{0\nu}|M^{0\nu}|^2\frac{\langle m_\nu\rangle^2}{m_e^2}, \tag{1}$$

where $G_{0\nu}|M^{0\nu}|^2\equiv F_N$ is a nuclear factor of merit and where $M^{0\nu}=M^{0\nu}_{\rm GT}-(g_V/g_A)^2M^{0\nu}_F$. The symbols $M^{0\nu}_F$ and $M^{0\nu}_{\rm GT}$ are, respectively, the dimensionless Fermi and Gamow-Teller nuclear matrix elements, g_V and g_A are the vector and axial-vector coupling constants, and $G_{0\nu}$ is the neutrinoless phase space integral. In the case of the ^{76}Ge neutrinoless decay, $G_{0\nu}=6.4\times10^{-15}\,{\rm yr}^{-1}$ [3]. The expression $\langle m_\nu\rangle=\Sigma_j\lambda_j m_jU^2_{ej}$ is the effective neutrino mass parameter, U_{ej} is the unitary matrix describing the mixing of j neutrinos to electron neutrinos, λ_j is a *CP* phase factor, and m_j is the neutrino mass eigenvalue.

Discovering neutrinoless decay would imply that $\langle m_\nu\rangle_{\rm expt}=m_e(F_NT^{0\nu}_{1/2})^{-1/2}$ eV, where m_e is the electron mass. Cancellation in the $\langle m_\nu\rangle_{\rm expt}$ expression may occur, but $\langle m_\nu\rangle_{\rm expt}\leqslant m_j^{\rm heaviest}$; i.e., at least one neutrino will have a mass not smaller than the value $\langle m_\nu\rangle_{\rm expt}$. Thus far, neutrinoless double-β decay has not been observed, and only an upper limit on $\langle m_\nu\rangle$ has been obtained from the measured lower limit of the half-life. In fact, $\langle m_\nu\rangle_{\rm expt}$ can be much smaller than individual neutrino masses. The factor F_N contains all of the nuclear physics and depends strongly on the nuclear model used; F_N can differ significantly from model to model as demonstrated in Table I. Therefore, having a hard bound on $T^{0\nu}_{1/2}$ does not justify placing a hard bound on $\langle m_\nu\rangle$, at least until the nuclear physics issues are resolved. The Heidelberg-Moscow result must also be interpreted with this caveat [4].

III. IGEX SETUP AND EXPERIMENTAL PARAMETERS

The International Germanium Experiment (IGEX) [5] is a search for the neutrinoless double-β ($\beta\beta$) decay of ^{76}Ge using a large amount of germanium (isotopically enriched to 86% in ^{76}Ge). The data presented here were previously collected in three laboratories: the Homestake gold mine [4000 meter of water equivalent (mwe)], the Canfranc Tunnel (2450 mwe), and the Baskan Neutrino Observatory (660 mwe). Three IGEX detectors of approximately 2-kg active mass each are currently operating in the new Canfranc Tunnel Laboratory, and the technology described in detail in this paper represents the present state of the art which will generate all future IGEX data. One detector of about 0.7-kg active mass has been operating in Baksan for several years and will soon be joined by two more similar detectors. A fourth 2-kg detector is planned for the Canfranc Laboratory. Earlier phases of the IGEX experiments have been described in several conference proceedings [5].

The summed energy of the two electrons from the neutrinoless double-β decay $^{76}{\rm Ge}\Rightarrow{}^{76}{\rm Se}+2e^-$ would appear as a peak at 2038.5 ± 0.4 keV [6] superimposed on the background spectrum. For maximum sensitivity, the experiment must have the lowest possible background, the best possible energy resolution, and the highest possible efficiency in this energy region of the spectrum. The best currently available technology meeting these criteria uses intrinsic germanium detectors, isotopically enriched in ^{76}Ge. IGEX has about 90 active moles of ^{76}Ge, a detection efficiency of almost 100%, and energy resolution of $\sim$0.15%. IGEX utilizes unique cryostat technology, ultralow background materials, archaeological lead shielding, and pulse-shape analysis to lower the background, which is the key to ultimate sensitivity.

All six IGEX detectors were grown and fabricated at Oxford Instruments, Inc., in Oak Ridge, Tennessee using germanium which was isotopically enriched in Russia to 86% in ^{76}Ge. The GeO_2 powder was purified, reduced to metallic form, and zone refined to $\sim10^{13}$ impurities per cubic centimeter by Eagle Picher, Inc., in Quapaw, Oklahoma. It was then shipped to Oxford by surface in order to minimize activation by cosmic ray neutrons [7], where it was further zone refined, grown into crystals, and fabricated into detectors.

All of the cryostat parts were electroformed onto stainless steel mandrels from a $CuSO_4$ solution. Data from the first three smaller detectors were analyzed, and small quantities of radium and thorium were observed. To reduce the thorium contamination, the $CuSO_4$ was purified by recrystallization. In this process, the copper sulfate crystals are dissolved in 18-MΩ water, and the solution is supersaturated by boiling. On cooling, copper sulfate recrystallizes from the solution. This results in a supernate of saturated copper sulfate and impurities. The supernate is removed by decantation. This process has been measured to reduce the thorium contamination by a factor greater than 200 in laboratory tracer studies. Sulfuric acid is the other major component of the plating bath. The highest purity acid commercially available, which came packaged in Teflon, was used. Radium was removed from the plating bath by the introduction of a barium scavenge ($BaSO_4$), which is trapped in the filtration system. The radium then readily exchanges with the barium during the normal online filtration process. The cryostats of all the large (2-kg) detectors were fabricated using these procedures.

The three large enriched (Rico Grande) detectors, designated RG-I, RG-II, and RG-III, have masses of 2150, 2194, and 2121 g, respectively. The dead layer thickness of RG-I was measured using the attenuated intensities of collimated ^{155}Eu gamma rays from 42 to 105 keV incident normal to the crystal. The measurements were made at various positions on the crystal and resulted in an average thickness of 0.5 mm. The active volumes of all three Rico Grande detectors were measured with a collimated source of ^{152}Eu in the Canfranc Laboratory. The corresponding active volumes were in good agreement with the standard Oxford efficiency measurements and also agreed with the active volume of RG-I as determined from the ^{155}Eu measurement above. All three detectors have active masses of $\sim$2 kg and efficiencies of $\sim$100% relative to a 7.62 cm$\times$7.62 cm cylindrical NaI(Tl) detector for 1333-keV gamma rays. These three detectors

contain a total of 67.9 active moles of ^{76}Ge.

The three smaller detectors produced during the first phase of IGEX were all cut from the same 4-kg crystal. They have total masses of 1006, 1018, and 896 g, respectively. The total active mass of the three detectors is ~2 kg or a total of ~22 mol.

The full width at half maximum (FWHM) energy resolutions of RG-I, RG-II, and RG-III, using the 1333-keV peak from a ^{60}Co source were 2.16, 2.37, and 2.13 keV, respectively. The energy resolution of the summed data presented here is interpolated from ^{208}Tl calibration lines to be ~4 keV at 2038 keV, the energy at which the 0ν $\beta\beta$-decay peak would appear. The counting rates of peaks in the background are currently so weak that they cannot be used to maintain energy calibration. Energy calibration and resolution measurements were made every 7–10 days using ^{22}Na, ^{60}Co, or natural thorium sources. The data from the three laboratories were combined after slight gain shifting to align the energy spectra at the 1460.75-keV background line from ^{40}K. The largest body of the data analyzed here was collected in the Homestake gold mine. Since the Homestake data were the least stable in gain, it was necessary to assign each pulse between 2020 and 2060 keV to an energy bin based on the position of the 2614-keV line from a ^{228}Th source measured before and after the relevant data collection period. On occasion, the calibration gain shifted excessively between the start and end of the counting period, and these data were not included in this analysis. These gain shift problems, which were possibly engendered by the environment of an operating gold mine, are far less prevalent in the Canfranc and Baksan laboratories.

The large detectors all have similar front-end electronics. The first-stage field-effect transistor (FET) is mounted on a Teflon block a few centimeters from the center contact of the crystal. The protective cover of the FET and the glass shell of the feedback resistor were removed to reduce radioactive background. This first-stage assembly is mounted behind a 2.5-cm-thick cylinder of archaeological lead to reduce background. Further stages of preamplification are located at the back of the cryostat crossarm approximately 70 cm from the crystal. The Rico Grande detectors now all have preamplifiers modified for pulse shape analysis.

The shielding of the Canfranc IGEX detectors (from inside to outside) is as follows. The innermost shield consists of 2.5 tons (~60 cm cube) of archaeological lead (2000 yr old) having a ^{210}Pb(^{210}Bi) content of <0.01 Bq/kg. The detectors fit into precision-machined holes in this central core, which minimizes the empty space around the detectors available to radon. Nitrogen gas, at a rate of 140 l per hour, evaporated from liquid nitrogen, is forced into the detector chambers to create a positive pressure and further minimize radon intrusion. The archaeological lead is centered in an ~1 m cube of 70-yr-old low-activity lead (~10 tons). A 2-mm-thick cadmium sheet surrounds the main lead shield, and two layers of plastic seal this central assembly against radon intrusion. A cosmic muon veto covers the top and two sides of the central passive core. The ends where the detector Dewars are located are not yet covered by active veto. It consists of BICRON BC-408 plastic scintillators 5.08 cm×50.8 cm ×101.6 cm with surfaces finished by diamond mill to optimize internal reflection. BC-800 (UVT) light guides on the ends taper to 5.08 cm in diameter over a length of 50.8 cm and are coupled to Hamamatsu R329 photomultiplier tubes. The anticoincidence veto signal is obtained from the logical ''OR'' of all photomultiplier tube discriminator outputs and reduces the background in the region of interest by about 40%. An external polyethylene neutron moderator 20 cm thick (1.5 tons) completes the shield. An external plastic tent, ''bubble room,'' surrounds the experiment, which is located in a room isolated from the rest of the laboratory, that is, 2450 mwe underground. The laboratory air is replaced every 4 h by forced ventilation from the main railway tunnel where there is a constant airflow. The overall result is a background of about $0.2c/\mathrm{keV\,kg\,yr}$ in the energy region between 2.0 and 2.5 MeV. This is expected to decrease even further as the cosmogenic activities in the detectors decay. The shieldings used in Homestake and Baksan are similar to that used in Canfranc with the exception that their innermost shields are 450-yr-old Spanish lead and copper stored underground for more than 20 yr respectively. There was no muon veto in Homestake, which was at 4000 mwe.

The data acquisition system now being used with the RG detectors in Canfranc is based on standard NIM electronics. The normal preamplifier output pulses from each detector are routed through two Canberra 2020 linear amplifiers having different shaping times to filter noise [8] and then are converted using Canberra 8701 Wilkinson type analog-to-digital converters (ADC's) controlled by PC's through parallel interfaces. The preamplifiers have been modified to optimize pulse shape discrimination by the addition of circuitry that extracts a ''charge collection detail signal'' (CCDS). Each preamplifier CCDS output is routed to either a LeCroy 9362 or 9360 digital oscilloscope, using a 1-MΩ 800-MHz active probe. The CCDS information is digitized at a rate of 2 ns per point and transferred to the computer via GPIB. For each event in a detector the following are recorded: (1) the arrival time, with a precision of 100 μs, (2) the elapsed time since the last veto event, (3) the energy from each ADC, and (4) the digitized CCDS wave form pulse-shape discrimination.

IV. BACKGROUND

The majority of the background currently comes from cosmic-ray neutron spallation reactions that occurred in the detector and cryostat components while they were above ground. The major contributions are from ^{68}Ge (271 d), ^{65}Zn (244 d), ^{56}Co (78 d), ^{57}Co (272 d), and ^{60}Co (1925 d), where the numbers in parentheses are the half-lives. Although these activities are decaying, the backgrounds from ^{60}Co and ^{68}Ge in the energy region of interest will not become negligible within the time frame of the experiment. Further background reduction requires pulse-shape analysis to discriminate double-β-decay events from these internal cosmogenic background events.

In large intrinsic Ge detectors, the electric field increases by a factor of more than 10 from the inner conductor to the outer conductor, which are almost 4 cm apart. Electrons and holes take 300–500 ns to reach their respective conductors. The current pulse contributions from electrons and holes are displacement currents, and therefore dependent on their velocities and radial positions. Accordingly, events occurring at

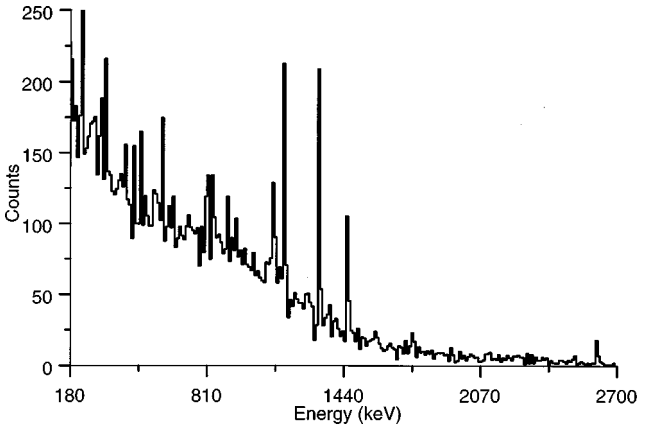

FIG. 1. A sample of the early data prior to gain shifting from all three 2-kg detectors. The spectrum is compressed to 10 keV per channel. The two peaks at 1173 and 1333 keV from ^{60}Co are dominantly from one detector (RG-II). This is thought to be a contaminant on some part of the cryostat, and steps to eliminate it will be taken.

a single site ($\beta\beta$-decay events for example) have associated current pulse characteristics that reflect the position in the crystal where the event occurred. More importantly, these single-site events frequently have pulse shapes that differ significantly from those due to the most dominant background events that produce electron-hole pairs at several sites by multi-Compton-scattering processes, for example. Pulse-shape analysis can be used to distinguish between these two types of energy depositions. Figure 1 shows a sample body of raw data that is a sum of early data collected from the three RG detectors and which has not been subjected to pulse shape analysis. The ^{60}Co lines were dominantly from a suspected contamination in the RG-II cryostat and are prime candidates for rejection using pulse-shape analysis.

An example characteristic of a single-site pulse is shown in Fig. 2(a). Figure 2(b) shows an example characteristic of a multisite event. For a complete description of the pulse-shape sorting technology, see Ref. [9]. Only a few events in the energy region of interest obviously resulting from multiple-site interactions in the crystal were removed from the data used here to place the lower bound on the half-life. Extensive experimental and computational studies are currently underway to significantly improve the efficiency of identifying multiple-site interactions and effectively remove the majority of them from future data sets.

The data from all IGEX detectors were gain shifted to the same energy scale. The portion of the composite spectrum relevant to $0\nu\ \beta\beta$ decay of ^{76}Ge is shown in Fig. 3; it represents 74.84 mol yr. The data are reported in 2-keV-wide bins because that is the smallest bin width that was used to record the earlier data. The energy resolution of the entire data set is 4 keV FWHM at 2038 keV. The data set between 2020 and 2060 keV is given in Table II. Less than 15% of the data contributing to this table have been subjected to pulse-shape discrimination, and only a small fraction of those events have been removed from the data set.

The current background without PSD averaged from 2.0 to 2.5 MeV is $\sim 0.20c$/keV kg yr and is lower than that represented in the data set analyzed here, which contains data

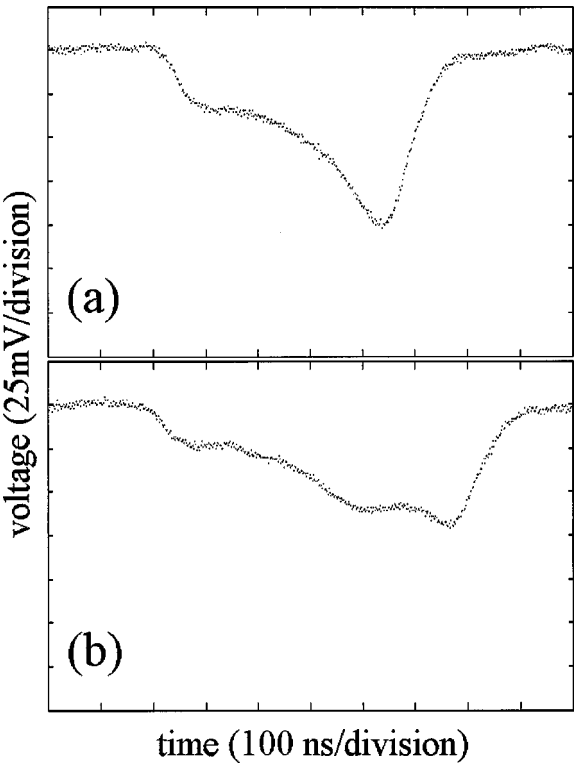

FIG. 2. (a) An example of a digitized charge collection detail signal preamplifier pulse from a single-site event. (b) An example from a multiple-site event. Each horizontal division represents 100 ns.

obtained while cosmogenic activities were still making significant contributions. Further background reduction is in progress through pulse-shape discrimination to eliminate multisite events. The current rudimentary PSD technology is capable of rejecting about two-thirds of the background events: so the present IGEX background is $\lesssim 0.06c$/keV kg yr with this PSD applied. Present efforts in preamplifier development and pulse-shape simulations are expected to significantly improve the background rejection efficiency.

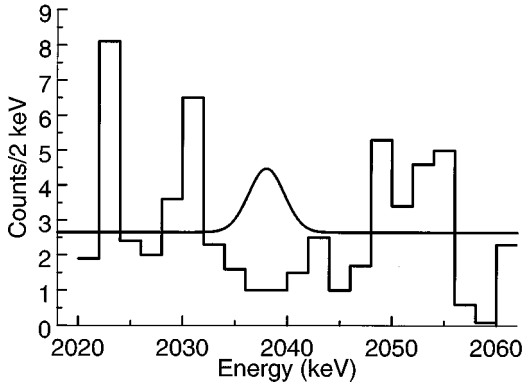

FIG. 3. A histogram of the early data in the energy region of interest for $0\nu\ \beta\beta$ decay representing 74.84 mol yr from all IGEX detectors. The base of the Gaussian resolution function has been shifted to the average background level between 2.0 and 2.5 MeV. The width of the Gaussian represents the experimental resolution, and the area under the Gaussian represents our adopted detection limit.

TABLE II. Data from six IGEX detectors representing 74.84 mol yr. The data were gain shifted to the same energy scale before summing. E (keV) is the lowest energy in each 2-keV bin. Approximately 15% of these data have been subjected to pulse-shape analysis; only a few obvious multisite events were removed.

E (keV)	Counts/2 keV	E (keV)	Counts/2 keV	E (keV)	Counts/2 keV
2020	1.9	2034	1.6	2048	5.3
2022	8.1	2036	1.0	2050	3.4
2024	2.4	2038	1.0	2052	4.6
2026	2.0	2040	1.5	2054	5.0
2028	3.6	2042	2.5	2056	0.6
2030	6.5	2044	1.0	2058	0.1
2032	2.3	2046	1.7	2060	2.3

The three RG detectors are now accumulating data with PSD pursuing the goal of probing Majorana neutrino masses corresponding to half-lives of 10^{26} yr.

V. RESULTS

The early data set in Table II was analyzed three different ways. First, the 1σ uncertainty in the number of events which could be contained in a Gaussian peak having FWHM $=4$ keV and centered at 2038 keV is 2.75. Therefore, the number of events attributable to 0ν $\beta\beta$ decay, C, is 4.53 at the 90% confidence limit. The product Nt corresponding to 74.84 mol yr is 4.51×10^{25} yr, and

$$T_{1/2}^{0\nu}\geqslant\frac{(\ln 2)Nt}{C}=\frac{3.12\times10^{25}\ \text{yr}}{4.53}=0.69\times10^{25}\ \text{yr}. \quad (2)$$

Next, an analytical maximum likelihood estimator [10] was applied over the 16-keV interval from 2030 to 2046 keV. Again, the detector response function was assumed to be a Gaussian with a FWHM$=4$ keV. Any energy interval used to compute the mean background yields a negative value for the most probable number of neutrinoless $\beta\beta$-decay events; hence, the value zero is assumed, in which case $C<4.0$ at the 90% confidence limit and $T_{1/2}^{0\nu}\geqslant0.78\times10^{25}$ yr.

Finally, we have also used the statistical estimator derived in a Poisson process recommended by the Particle Data Group [11]. Using this method, $C\leqslant3.84$ at the 90% confidence limit. This is equivalent to $T_{1/2}^{0\nu}\geqslant0.81\times10^{25}$ yr.

We have adopted from these estimators the value $T_{1/2}^{0\nu}\geqslant0.8\times10^{25}$ yr; however, Table II contains all of the raw data in the energy region of interest and can be interpreted by the reader using any analytical formalism to verify the legitimacy of the above value. The curve in Fig. 3 represents the upper bound of neutrinoless $\beta\beta$ counts leading to the above half-life at the 90% confidence limit.

To deduce a limit on the neutrino mass parameter from the above experimental bound on the half-life, a reliable nuclear matrix element is required. A large number of nuclear matrix elements have been calculated in the shell model [12, 13] and with the quasirandom phase approximation (QRPA) method [14–17]. In the QRPA, the 2ν $\beta\beta$-decay theoretical nuclear matrix elements exhibit an extreme sensitivity to the choice of nuclear parameters, for example, the particle-particle force parameter g_{pp}. In the case of 0ν $\beta\beta$ decay, the nuclear matrix elements are far less sensitive to the choice of parameters; however, there are still significant differences between the results of the various calculations as shown in Table I. Recent large model-space shell model calculations for ^{76}Ge [13] result in a nuclear factor of merit F_N about 10 times smaller than that computed in the weak coupling shell model [12] and in the QRPA method of Refs. [16] and [17], although it is rather similar to the first QRPA calculation of Ref. [14], which used a simple schematic interaction. Table I gives the ^{76}Ge nuclear factor of merit computed using the various nuclear models.

The extraction of the neutrino mass parameter $\langle m_\nu\rangle$ from the bound on the half-life is therefore not straightforward as can be appreciated by referring to Table I where upper bounds range from 0.46 to 1.9 eV based on the IGEX data. The question of nuclear structure is still an open one. A more stringent limit of $T_{1/2}^{0\nu}\geqslant1.1\times10^{25}$ yr at the 90% C.L. has been recently reported by the Heidelberg-Moscow group [4].

Obtaining the ultimate sensitivity from large, isotopically enriched ^{76}Ge experiments requires the perfection of pulse-shape discrimination techniques. Presently, only pulses with shapes that are obviously characteristic of multiple interactions in the crystal are being removed from the data. This results in a significant number of background events remaining in the data set. A two-pronged program to further eliminate background events, consisting of computational pulse-shape simulations and further development of the electronic system, is underway in IGEX. The goal is to maintain, with a high degree of confidence, only pulses that are from single-site interactions and to accurately determine the fraction of all single-site interactions rejected.

ACKNOWLEDGMENTS

The Canfranc Astroparticle Underground Laboratory is operated by the University of Zaragoza under Contract No. AEN96-1 657. This research was partially funded by the Spanish Commission for Science and Technology (CICYT), the U.S. National Science Foundation, and the U.S. Department of Energy. The isotopically enriched ^{76}Ge was supplied by the Institute for Nuclear Research (INR), Moscow, and the Institute for Theoretical and Experimental Physics (ITEP), Moscow.

[1] J. Schechter and J. W. F. Valle, Phys. Rev. D **25**, 2951 (1982).
[2] B. Kayser, in *Proceedings of the XXIII International Conference on High Energy Physics*, edited by S. C. Loken (World Scientific, Singapore, 1987), p. 951; S. P. Rosen, in *Symmetries and Fundamental Interactions in Nuclei*, edited by Wick C. Haxton and Ernest M. Henley (World Scientific, Singapore, 1995), p. 251.
[3] M. Doi, T. Kotani, and E. Takasugi, Prog. Theor. Phys. Suppl. **83**, 1 (1985).
[4] L. Baudis *et al.*, Phys. Lett. B **407**, 219 (1997).
[5] F. T. Avignone III *et al.*, Nucl. Phys. B (Proc. Suppl.) **35**, 354 (1994); C. E. Aalseth *et al.*, *ibid.* **48**, 223 (1996); C. E. Aalseth *et al.*, in *Proceedings of the XVII International Conference on Neutrino Physics and Astrophysics* (Neutrino 96), edited by K. Enqvist, K. Huitu, and J. Maalampi (World Scientific, Singapore, 1997), p. 361.
[6] V. I. Tetyak and Yu. Zdesenko, At. Data Nucl. Data Tables **61**, 43 (1995).
[7] F. T. Avignone *et al.*, Nucl. Phys. B (Proc. Suppl.) **28A**, 280 (1992).
[8] J. Morales *et al.*, Nucl. Instrum. Methods Phys. Res. A **231**, 410 (1992).
[9] C. E. Aalseth, F. T. Avignone, R. L. Brodzinski, H. S. Miley, and J. H. Reeves, J. Radioanal Nucl. Chem. **233**, 119 (1998).
[10] F. T. Avignone III, Nucl. Instrum. Methods Phys. Res. A **245**, 525 (1986).
[11] R. M. Barnett *et al.*, Phys. Rev. D **54**, 155 (1996).
[12] W. C. Haxton and G. J. Stephenson, Jr., Prog. Part. Nucl. Phys. **12**, 409 (1984); W. C. Haxton, Nucl. Phys. B (Proc. Suppl.) **31**, 82 (1993).
[13] E. Caurier *et al.*, Phys. Rev. Lett. **77**, 1954 (1996); P. B. Radha *et al.*, *ibid.* **76**, 2642 (1996).
[14] P. Vogel and M. R. Zirnbauer, Phys. Rev. Lett. **57**, 3148 (1986); J. Engel, P. Vogel, and M. R. Zirnbauer, Phys. Rev. C **37**, 731 (1988).
[15] M. K. Moe and P. Vogel, Annu. Rev. Nucl. Part. Sci. **44**, 247 (1994).
[16] O. Civitarese, A. Faessler, and T. Tomoda, Phys. Lett. B **194**, 11 (1987); T. Tomoda, Rep. Prog. Phys. **54**, 53 (1991) and references therein.
[17] K. Muto and H. V. Klapdor, Phys. Lett. B **201**, 420 (1988); A. Staudt, K. Muto, and H. V. Klapdor-Kleingrothaus, Europhys. Lett. **13**, 31 (1990).